

Corrosion Inhibition Performance of a Novel Cationic Surfactant for protection of Carbon Steel Pipeline in Acidic Media

M.A. Hegazy¹, M. Abdallah^{2,3,*}, M. Alfakeer⁴, H. Ahmed³

¹ Egyptian Petroleum Research Institute (EPRI), Nasr City, Cairo, Egypt

² Chemistry Department, Faculty of Applied Sciences, Umm Al-Qura University, Makkah, Saudi Arabia

³ Chemistry Dept., Faculty of Science, Benha University, Benha, Egypt

⁴ Chemistry Dept., Faculty of Science, Princess Nourah bint Abdulrahman University -Riyadh, Saudi Arabia

*E-mail: metwally555@yahoo.com

Received: 18 March 2018 / Accepted: 6 May 2018 / Published: 5 June 2018

The corrosion inhibiting action of a novel cationic surfactant on the dissolution of carbon steel (C-steel) in 1M HCl has been investigated using weight loss, electrochemical impedance spectroscopy and potentiodynamic polarization techniques. The effect of inhibitor concentration and temperature on the corrosion rate of C-steel was determined from weight loss approach. While the electrochemical and potentiodynamic measurements were used to explain the behavior of C-steel at a temperature 20 °C. Adsorption of the cationic surfactant on the surface of the C-steel pipeline is a mixture of physical and chemical adsorption and obeys Langmuir isotherm. The thermodynamic data of activation and adsorption were calculated and explained.

Keywords: C-steel; cationic surfactant, Adsorption; corrosion inhibitors; Interfaces

1. INTRODUCTION

C-steel is used in many fields such as building materials for pipe work in oil and gas production such as tubular hole down, pipe tubes and conveying tubes [1]. Oil well stimulation, usually done with hot solutions of HCl, resulting in a severe corrosion attack on the production pipes, bottom hole tools and casing. Stimulating oil wells is what describes a variety of processes that are done to improve well production. Open new channels in the oil and gas rock to flow through the so-called stimulation [2]. In order to diminish the impact of corrosion on industrial facilities, many ways were applied. However, it is one of the best ways to protect metals from corrosion damage is the application of corrosion inhibitors [3-8]. These inhibitors can be organic or inorganic origin. There are many compounds such

as chromates and nitrite give high inhibition corrosion efficiency but unfortunately these compounds are toxic and dangerous to the environment, and there are warnings about their use. Therefore, many attempts to find alternatives to similar activity or better inhibitory and friendly to the environment [9]. The capacity of organic compounds as corrosion inhibitors depend on the amount of adsorption and the amount of the covered part of the metal surface [10-15].

It was found that adsorption of organic inhibitors depended on the molecular structure of the inhibitor, the presence of active surface in their structure, charge of the metal used, and type of corrosive electrolytes [16]. The adsorption process on the surface of the electrode is stimulated by the presence of hydrophilic and hydrophobic groups in the chemical structure of the inhibitor [17,18]. Thus, the application of compounds that have surface activity as corrosion inhibitors consisting of one hydrophilic head group and one hydrophobic chain have been extensively studied [19-25]

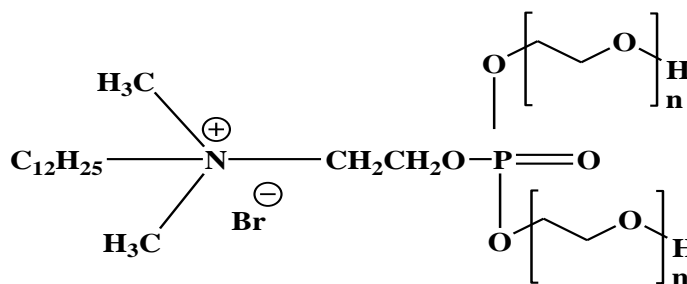
It has been reported that quaternary ammonium compounds are important as corrosion inhibitors in hydrochloric acid [26]. The concentration effect, functional groups and halide ions of the quaternary ammonium inhibitors have been extensively studied for the inhibition of corrosion of steel. The addition of halide ions to organic cations as a synergistic effect leads to improved inhibition efficiency [27]. Literature indicated that the long chain alkyl quaternary ammonium compounds are good inhibitors for corrosion of steel in acidic solutions [28]

The goal of this manuscript is to study the adsorption and the inhibition effect of C-steel corrosion in 1M HCl solution using weight loss, potentiodynamic polarization and electrochemical impedance spectroscopy measurements. The thermodynamic parameters of the adsorption of the cationic surfactant on the C-steel surface were also investigated

2. EXPERIMENTAL METHODS

2.1. Synthesis of cationic surfactant

The synthesis of cationic surfactant takes place in three steps. Firstly, the quaternization reaction of 1-bromododecane with an appropriate amount of 2-(dimethylamino) ethanol in the molar ratio of 1:1 to produce N-(2-hydroxyethyl)-N,N-dimethyldodecan-1-aminium bromide, [29]. Reactant substances have been allowed to reflux in ethanol for 12 h. Then leave the reaction mixture to cool down at room temperature. The precipitate was purified by ether, then crystallized from ethanol. In the second step, the esterification reaction of ammonium tetrachloride salt synthesis and phosphoric acid in the presence of toluene as a solvent and p-toluene sulfonic acid as a drying agent [29] in the molar ratio of 1: 1 to produce N-dodecyl-N,N-dimethyl-O-(2-phosphonoethyl)hydroxylammonium bromide. The reaction was completed when the water was removed from the reaction system. The reaction mixture was distilled under vacuum to completely remove the solvent. In the third step, the product of the second step and polyethylene glycol were esterified as described in the second step in the molar ratio of 1: 2 to produce N-(2-((bis((26-hydroxy-3,6,9,12,15,18,21,24-octaohexacosyl)oxy)phosphoryl)oxy)ethyl)-N,Ndimethyldodecan-1-aminium bromide. The chemical structure of the synthesized inhibitor (**Fig. 1**) was characterized by FTIR, ¹HNMR, and ³¹PNMR spectroscopic analyses.



***N*-(2-((bis(polyethyleneglycol)phosphoryl)oxy)ethyl)-*N,N*-dimethyldodecan-1-aminium bromide**

Figure 1. Chemical structure of the synthesized novel cationic surfactant.

2.2. Materials

In this study, C-steel specimens were used with the following chemical composition (wt.%): 0.19% C, 0.94% Mn, 0.022% Cu, 0.014% Ni, 0.016% V, 0.05% Si, 0.034% Al, 0.009% Cr, 0.009% P, 0.004% S, 0.003% Ti and the rest is Fe. All the solutions used in this manuscript were freshly prepared from Aldrich chemicals using bidistilled water. Stock solutions of HCl solution were prepared using bidistilled water. The inhibitor solutions were prepared by dissolving the required amount of the cationic surfactant in bidistilled water and the desired concentrations were obtained by appropriate dilution.

2.3. Weight loss measurements

The C-steel specimens with a dimension of 5 cm x 3cm x 0.4 cm polished with a different grades of emery paper and then washed with distilled water and acetone. After weighing accuracy, the specimens were submerged in a beaker containing 100 ml of 1 M HCl solution devoid of and containing different concentrations of the synthesized inhibitor at various temperatures in the range 20–80°C. The temperature was controlled by water bath provided with a thermostat control $\pm 1^\circ\text{C}$. C-steel samples were taken after 24 hours. Rinse with distilled water twice and degreased with acetone. After the samples were immersed in 1 M HCl solution for 10 seconds (chemical method to clean the rust products), rinse twice with twice distilled water, dried, and carefully weighted. Trials were conducted in three versions. The tests were repeated at different temperatures.

2.4. Electrochemical measurements

Potentiodynamic polarization experiments were performed using a cell containing three electrodes, platinum counter electrode (CE) and a saturated calomel electrode (SCE) and working electrode (WE). WE used in the experiments is a cylindrical C-steel rod embedded in Araldite with an exposed surface area of 0.42cm^2 . The treatment of the electrode as described in the weight loss measurements. Potentiodynamic polarization measurements were obtained by changing the electrode

potential automatically from -850 to -350 mV vs. SCE at open circuit potential with a scan rate 2 mV s^{-1} at $20 \text{ }^\circ\text{C}$. Electrochemical impedance spectroscopy experiments were performed as explained before [30]. A small alternating voltage perturbation (5 mV) was imposed on the cell over the frequency range of 100 kHz–30 mHz at $20 \text{ }^\circ\text{C}$.

3. RESULTS AND DISCUSSION

3.1. Confirmation the chemical structure of the cationic surfactant

3.1.1. FTIR spectra

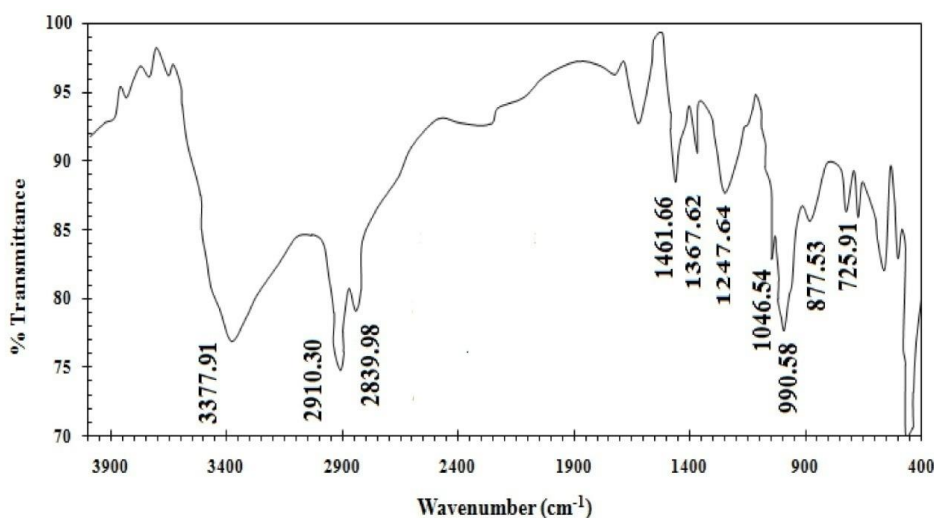


Figure 2. FTIR of cationic surfactant.

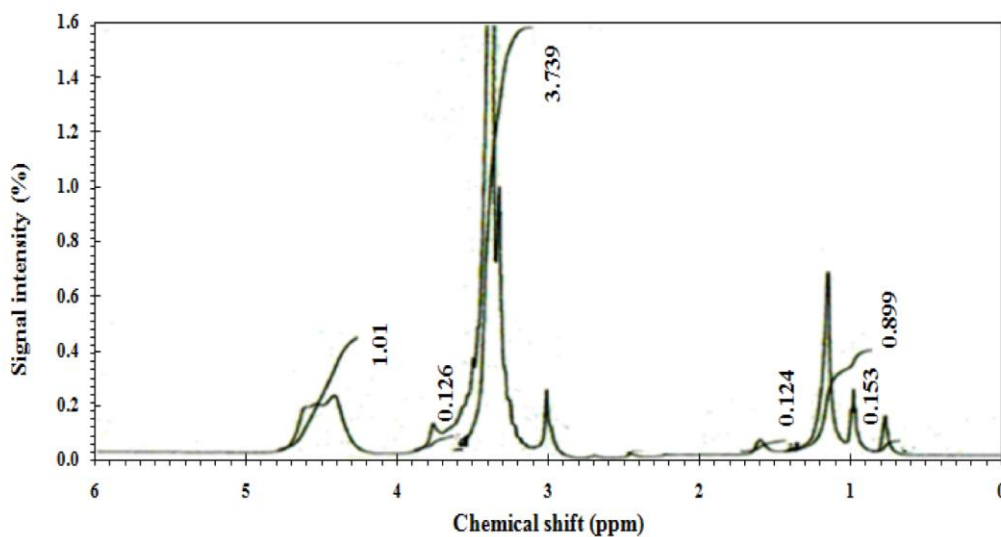


Figure 3. ¹H NMR of cationic surfactant

FTIR spectrum showed that the distinctive bands for the alkyl part were at 2910.30 and 2839.98 cm^{-1} for asymmetric and symmetric stretching (CH), respectively. Whereas, they were observed at 1333.06 cm^{-1} for symmetric bending (CH_3), at 1461.66 cm^{-1} for symmetric bending (CH_2), and at 725.91 cm^{-1} for $-(\text{CH}_2)_n-$ rock. C–O stretching band 1247.64 cm^{-1} , C–N⁺ at 1046.54 cm^{-1} , P–O–C at 990.58 cm^{-1} , 3377.91 cm^{-1} was due to stretching OH. FTIR spectra confirmed the expected functional groups in the synthesized compound as shown in Fig. 2.

3.1.2. ¹H NMR spectra

The ¹H NMR spectrum of the synthesized compound showed different bands at $\delta = 0.7832$ – 0.9973 ppm (t, 3H, $\text{NCH}_2\text{CH}_2(\text{CH}_2)_n\text{CH}_3$); $\delta = 1.0107$ – 1.1731 ppm (m, 18H, $\text{NCH}_2\text{CH}_2(\text{CH}_2)_n\text{CH}_3$); $\delta = 1.6109$ ppm (m, 2H, $\text{NCH}_2\text{CH}_2(\text{CH}_2)_n\text{CH}_3$); $\delta = 3.0292$ – 3.5778 ppm (m, 24 H, $\text{POCH}_2\text{CH}_2\text{N}$); $\delta = 4.4323$ – 4.6177 ppm (m, 6H, $\text{NCH}_2\text{CH}_2\text{POCH}_2\text{CH}_2\text{O}$); $\delta = 3.7747$ ppm (s, 1H, $\text{POCH}_2\text{CH}_2\text{OH}$) as shown in Fig. 3.

³¹P NMR spectra

³¹P NMR (DMSO-d₆) spectrum of the compound showed characteristic δ_p signal at 4.4680–19.5401 ppm as shown in Fig. 4.

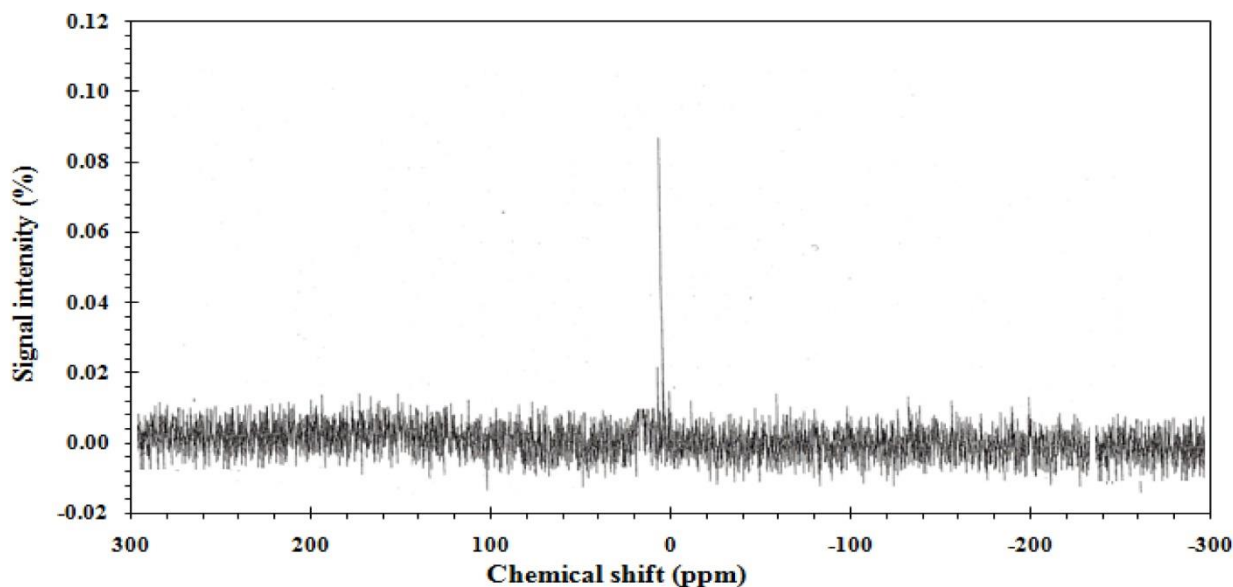


Figure 4. ³¹P NMR of cationic surfactant.

3.2. WL measurement

3.2.1. Effect of cationic surfactant concentration

The corrosion rate (k) was computed from the next equation [31].

$$k = \frac{\Delta W}{At} \tag{1}$$

where (ΔW) the average weight loss, (A) is the surface area in cm^2 and (t) is the time in hours. Corrosion rate values of C-steel in 1 M HCl solution are shown in the absence and presence of various concentrations of the cationic surfactant in Table 1. Inspection of this Table, it is observed that, the value of k decreases with the increased concentration of the cationic surfactant. Corrosion inhibition gradually increased by increasing the inhibitor concentration.

The inhibition efficiencies (η_w) of the C-steel in 1 M HCl solution devoid of and containing the different concentrations of cationic surfactant are calculated according to the following equation [32].

$$\eta_w = \frac{(k_{free} - k_{inh})}{k_{free}} \times 100 \tag{2}$$

where k_{free} and k_{inh} the corrosion rate of the C-steel in 1 M HCl solution devoid of and containing various concentrations of cationic surfactant, respectively.

More inspection of Table 1 revealed that, the values of η_w increase with increasing the concentrations of cationic surfactant.

Table 1. Corrosion rate of C-steel surface coverage and percentage inhibition efficiency for C-steel in 1M HCl in the absence and presence of different concentrations of cationic surfactant from weight loss measurements at different temperatures

Conc. of inhibitor M	20 °C			40 °C			60 °C			80 °C		
	K mg cm^{-2} h^{-1}	Θ	η_w %	k mg cm^{-2} h^{-1}	Θ	η_w %	k mg cm^{-2} h^{-1}	Θ	η_w %	k mg cm^{-2} h^{-1}	Θ	η_w %
0.00	0.4192	0.00	0.00	1.6996	--	--	5.7325	--	--	16.0965	--	--
5×10^{-5}	0.0692	0.83	83.50	0.2719	0.84	84.00	0.9057	0.84	84.20	2.5754	0.84	84.00
1×10^{-4}	0.0582	0.86	86.12	0.2260	0.87	86.70	0.7555	0.87	86.82	2.1376	0.87	86.72
5×10^{-4}	0.0389	0.91	90.71	0.1533	0.91	90.98	0.5325	0.91	90.71	1.4954	0.91	90.71
1×10^{-3}	0.0327	0.92	92.19	0.1292	0.92	92.40	0.4454	0.92	92.23	1.2684	0.92	92.12
5×10^{-3}	0.0224	0.95	94.66	0.0869	0.95	94.89	0.3066	0.95	94.65	0.8836	0.95	94.51

3.2.2. Effect of temperature

The influence of rising temperature on the η_w obtained by weight loss of the C-steel was evaluated in the absence and presence of different concentration of cationic surfactant in 1.0 M HCl solution are represented in Fig. 5. Inspection of this figure and the data in Table 1 clarified that, as the temperature rises, the amount of weight loss increases. The increase of corrosion rate due to an accelerating factor of temperature, which increases the energy of the reacted species, as a result, chemical reactions get much faster [33].

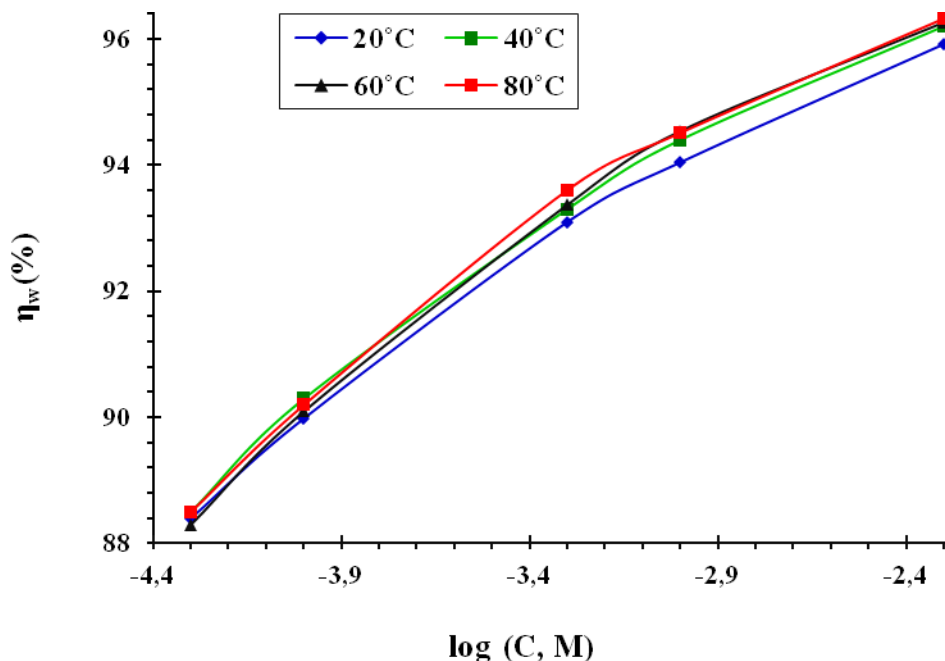


Figure 5. Effect of temperature on the inhibition efficiency obtained by a weight loss method for C-steel in 1 M HCl in the presence of different concentrations of cationic surfactant.

The worthless changing of the value η_w with increasing temperature may mention to the vigorous adsorption of the cationic surfactant on C-steel surface [34]. Therefore, the C-steel surface is effectively protected from the hydrochloric corrosion solution by forming the adsorption film [35].

3.2.3. Kinetic parameters

Thermodynamic activation parameters such as energy activation (E_a), enthalpy (ΔH^*), and entropy (ΔS^*) of activation have an important role in understanding the mechanism of inhibition by organic compounds. The activation energy values (E_a) were calculated from the Arrhenius equation as follows [36]:

$$\ln k = \frac{-E_a}{RT} + \ln A \tag{3}$$

where, k is the rate of C-steel corrosion, A is the frequency factor, and R is the universal gas constant.

Figure 6 shows a plot of $\ln k$ against $1/T$ of C-steel corrosion in 1 M HCl solution in the absence and presence of different concentrations of cationic surfactants is presented in Fig.6. The linear curve was obtained with slope equal $(-E_a / R)$. The values of E_a , was calculated and included in Table 2 it is clear that the values of E_a are less or no change compared to the blank. The low or no change in the activation energy value in the presence inhibitor compared with that in its absence is attributed to its chemisorption, whereas the reverse is the case with physical adsorption [37].

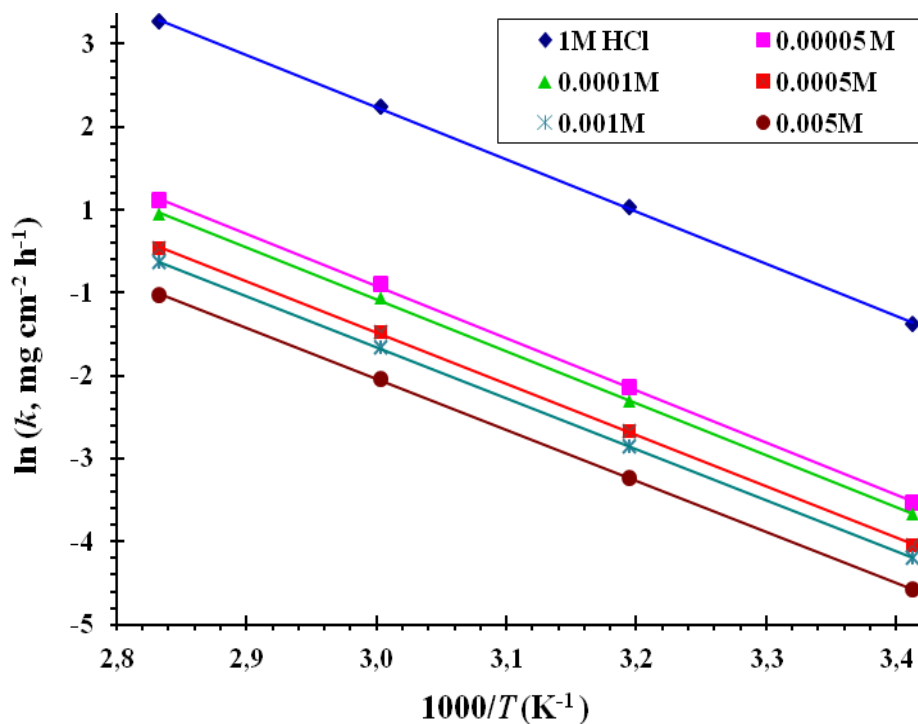


Figure 6. $\ln k$ vs. $1/T$ curves for C-steel dissolution in absence and presence of different concentrations of cationic surfactant in 1 M HCl solution

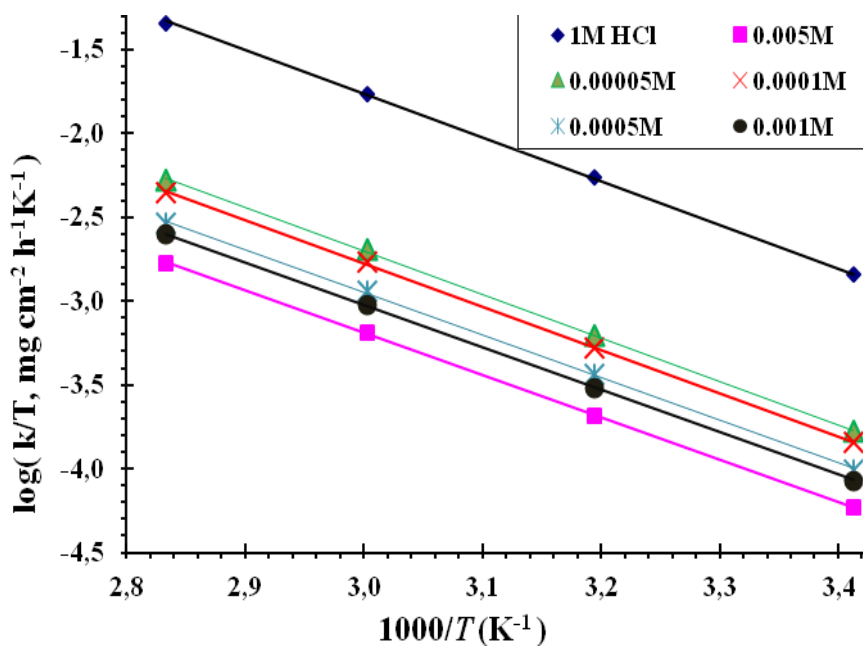


Figure 7. Relationship between $\log k/T$ and the reciprocal of the absolute temperature of C-steel in 1M HCl.

In order to calculate the enthalpy, ΔH^* and entropy, ΔS^* of activation of the corrosion process, the alternative formula of Arrhenius equation, also called the transition state equation was used [38]:

$$\ln\left(\frac{k}{T}\right) = \left(\ln\left(\frac{R}{N_A h}\right) + \left(\frac{\Delta S^*}{R}\right)\right) - \frac{\Delta H^*}{RT} \quad (4)$$

where h is the Planck's constant, N is the Avogadro's number, T is the absolute temperature and R is the universal gas constant.

The plots of $\ln(k/T)$ versus $1/T$, were given straight lines as shown in Fig.7 for C-steel dissolution in 1 M HCl solution in the absence and presence of different concentrations of cationic surfactant. Straight lines are obtained with a slope of $(-\Delta H^*/R)$ and an intercept of $\ln((R/Nh) + \Delta S^*/R)$. The values of ΔH^* and ΔS^* are shown in Table 2. The positive values of ΔH^* in the absence and presence of inhibitor reflect the endothermic nature of the C-steel dissolution process and indicates that the dissolution of C-steel is difficult. Table 2 also shows that the values of E_a and ΔH^* are vary in the same manner. This result allows to verify the known thermodynamic reaction between the E_a and ΔH^* equation (5) [39] But the values of ΔH^* are lower than the E_a value. This has been reported [40] to indicate that the corrosion process must involve a gaseous reaction, simply a hydrogen evolution reaction associated with a decrease in the total reaction volume.

$$\Delta H_a = E_a - RT \quad (5)$$

The values of ΔS^* in the absence and presence of the synthesized cationic surfactant are negative (Table2) This indicates that the activated complex in the rate determining step represents an association rather than dissociation meaning that a decrease in disordering takes place on going from reactants to activate complex.

Table 2. Values of activation parameters for C-steel in 1 M HCl in absence and presence of different concentrations of the synthesized cationic surfactant

Conc. of inhibitor M	E_a kJ mol ⁻¹	ΔH^* kJ mol ⁻¹	ΔS^* J mol ⁻¹ K ⁻¹	$E_a - \Delta H^*$ kJ mol ⁻¹
0.00	52.36	49.70	-156.08	2.66
5×10^{-5}	51.88	49.23	-260.82	2.66
1×10^{-4}	51.72	49.06	-273.45	2.66
5×10^{-4}	52.47	49.81	-278.45	2.66
1×10^{-3}	52.54	49.89	-285.92	2.66
5×10^{-3}	52.87	50.21	-299.37	2.66

3.3. Adsorption isotherm and the mechanism of inhibition

Generally, the mechanism of inhibition of corrosion of C-steel in HCl solution in the presence of cationic surfactant is the adsorption of it at the C-steel /solution interface

For the inhibitory process, it is generally assumed that the absorption of cationic surfactant molecules on C-steel surfaces cannot be considered pure physical or purely chemical absorption. The value of inhibitory efficiency depends on several factors; such as the occurrence of some active center in the chemical composition of the inhibitor to accelerate the adsorption process, the nature of the electrode and the corrosive solution used, the charge density, molecular size, temperature, reaction and ability of the inhibitor to form complexes with metal ions[41].The important information about the interaction between the cationic surfactant and the C-steel surface can be interpreted by adsorption isotherm. The degree of surface coverage (θ) for different concentrations of cationic surfactant in 1.0 M HCl was evaluated by weight loss equation (3) [39]:

$$\theta = \frac{(k_{free} - k_{inh})}{k_{free}} \tag{6}$$

So far, the best results are provided by application of Langmuir isotherm and it can be can be applied using the following equation: [43]

$$\frac{C}{\theta} = \frac{1}{K_{ads}} + C \tag{7}$$

where C is the concentration of the cationic surfactant compound, and K_{ads} is the equilibrium constant of adsorption. **Figure 8** represents the relation between C/θ and C . A straight line was obtained with the slope clothed to unity indicating the adsorption of cationic surfactant on the C-steel surface obeys Langmuir isotherm [43]. From these results one can assume that there is no interaction between the adsorbed species.

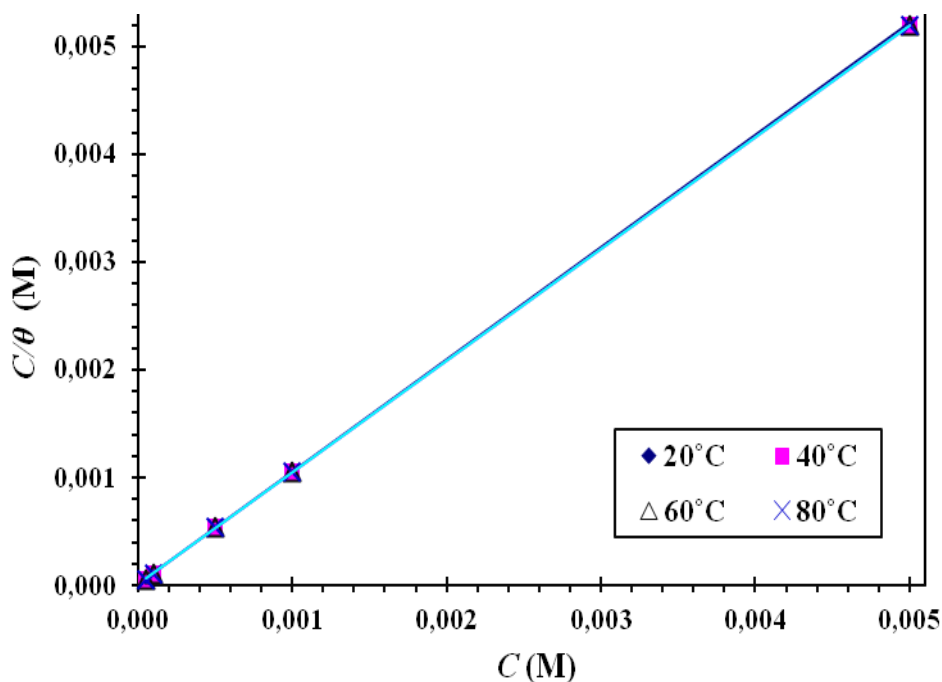


Figure 8. Langmuir adsorption isotherm for the cationic surfactant adsorbed on C-steel surface in 1 M HCl at different temperatures.

Furthermore, the basic attribute of Langmuir isotherm can be elucidated in the term of a dimensionless separation factor, R_L [43], which describe the type of isotherm and its definition by:

$$R_L = \frac{1}{1 + K_{ads}C} \quad (8)$$

The low value of R_L suggest a highly appropriate adsorption. If $R_L > 1$ inappropriate, $R_L = 1$ linear, $0 < R_L < 1$ appropriate, and if $R_L = 0$ irreversible.

Table 3 gives the determined value of R_L for various concentrations of the cationic surfactant. The value of R_L was found to be less than unity indicating that adsorption processes were appropriate.

Table 3. Values of dimensionless separation factor, R_L , and other thermodynamic parameters of adsorption on C-steel surface in 1 M HCl containing different concentrations of the synthesized cationic surfactant

Temperature °C	Conc. of inhibitor M	R_L	y	$K_{Kinetic}$
20	5×10^{-5}	0.2605	0.2731	7.97×10^6
	1×10^{-4}	0.1498		
	5×10^{-4}	0.0340		
	1×10^{-3}	0.0173		
	5×10^{-3}	0.0035		
40	5×10^{-5}	0.2571	0.2729	9.24×10^6
	1×10^{-4}	0.1475		
	5×10^{-4}	0.0335		
	1×10^{-3}	0.0170		
	5×10^{-3}	0.0034		
60	5×10^{-5}	0.2543	0.2587	1.37×10^7
	1×10^{-4}	0.1456		
	5×10^{-4}	0.0330		
	1×10^{-3}	0.0168		
	5×10^{-3}	0.0034		
80	5×10^{-5}	0.2514	0.2559	1.43×10^7
	1×10^{-4}	0.1437		
	5×10^{-4}	0.0325		
	1×10^{-3}	0.0165		
	5×10^{-3}	0.0033		

The experimental data have been then fitted into the modified form of the Langmuir isotherm which known as El-Awady kinetic–thermodynamic adsorption model, which may adequately represent the adsorption behavior of the cationic surfactant on the C-steel surface. El–Awady isotherm is represented by the following equation [44]:

$$\ln\left(\frac{\theta}{1-\theta}\right) = \ln K' + y \ln C \quad (9)$$

where, K' is a constant, and y is the number of inhibitory molecules occupying one active site. The plot of $\ln(\theta/1-\theta)$ versus $\ln(C)$ gives a straight line of slop y and the intercept of $\ln(K')$, as

shown in **Fig.9**. The equilibrium constant corresponding to adsorption isotherm is given by the following equation:

$$K = K^{1/y} \tag{10}$$

where y denotes the number of inhibitor molecules occupying a given position. The value of $y > 1$ means a multi-layer formation of the inhibitor on the metal surface.

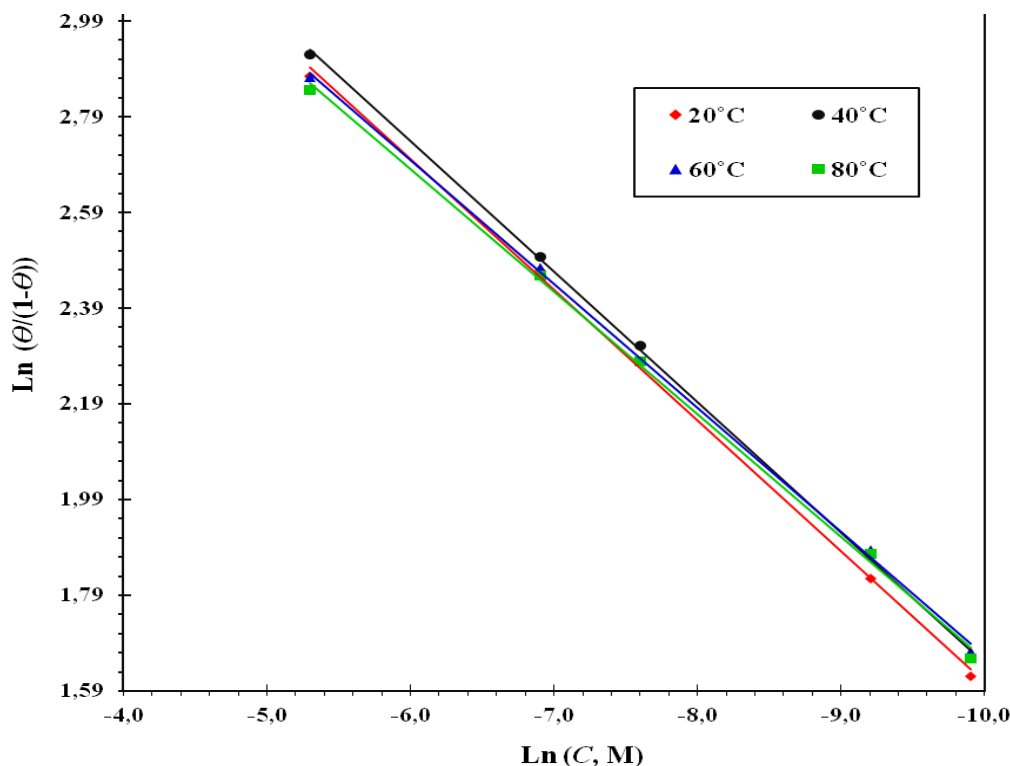


Figure 9. Kinetic–thermodynamic model for the adsorption of cationic surfactant in 1M HCl solution on C-steel.

The value of $y < 1$ means a certain inhibitor molecule occupies more than one active site. The value of y was less than the unit indicating the assumptions of the Langmuir adsorption isotherm. The behavior of the equilibrium constants acquired from the Langmuir model was analogous to the values acquired by kinetic-thermodynamic model. The values of K_{ads} , indicating the binding force of the cationic surfactant on the surface of the C-steel and leads to calculate the free energy of adsorption ΔG°_{ads} , using the following equation [45]:

$$\Delta G^{\circ}_{ads} = -RT \ln (55.5 K_{ads}) \tag{11}$$

where R is the molar gas constant, T is the absolute temperature and 55.5 is the concentration of water in solution expressed in mol dm^{-3} .

The calculated ΔG°_{ads} values are given in Table 4. It is clear that from these values, the adsorption mechanism of cationic surfactant on the C-steel surface from in 1 M HCl solution is mixed physical and chemical adsorption but chemical adsorption is more than physical one [26].

Furthermore, the values of the enthalpy ΔH°_{ads} and Entropy ΔS°_{ads} of adsorption were computed using the following equation [46]:

$$\Delta G^{\circ}_{ads} = \Delta H^{\circ}_{ads} - T\Delta S^{\circ}_{ads} \quad (12)$$

A plot of ΔG°_{ads} versus T gave a straight line (Fig.10) with a slope of $-\Delta S^{\circ}_{ads}$ and an intercept of ΔH°_{ads} .

The values of thermodynamic parameters for the adsorption of cationic surfactant in 1 M HCl solution on the surface of C-steel are given in Table 4.

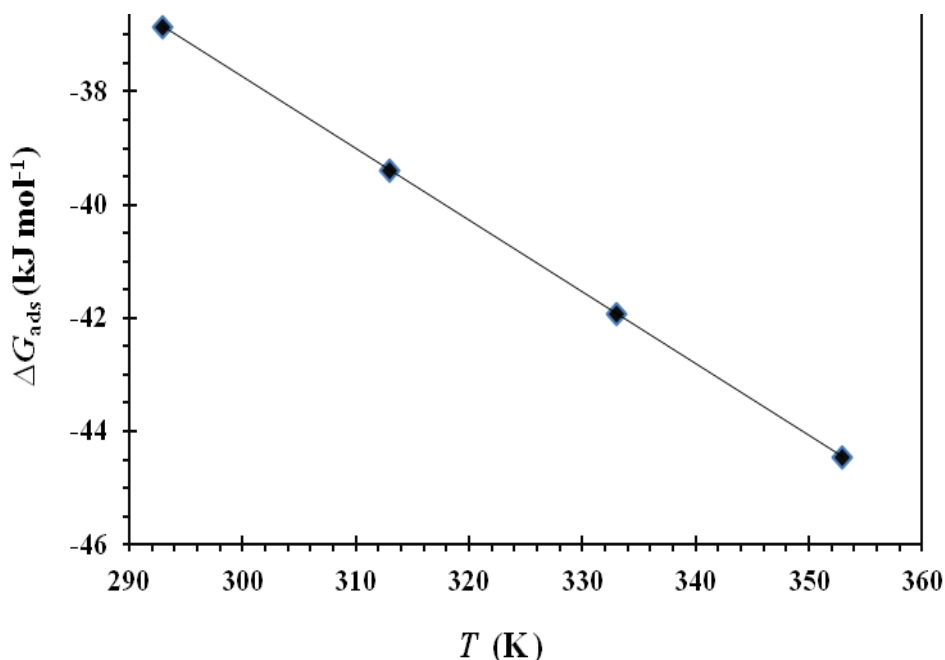


Figure 10. Relationship between ΔG°_{ads} and T of C-steel in absence and presence of different concentrations of cationic surfactant in 1 M HCl solution.

The obtained value of ΔH°_{ads} is positive this means that the adsorption of cationic surfactant molecules onto the C-steel surface is an endothermic process, which is attributable unequivocally to chemisorption [47,48].

The positive value obtained from ΔS°_{ads} indicates that the adsorption of cationic surfactant from the aqueous electrolyte can be considered as replacement process between the inhibitor in the aqueous electrolyte and the water molecules on the surface of the C-steel[49].

Table 4. Thermodynamic parameters of adsorption on C-steel surface in 1 M HCl containing different concentrations of the synthesized cationic surfactant

Temperature °C	$K_{ads} \times 10^{-4}$ M ⁻¹	ΔG°_{ads} kJ mol ⁻¹	ΔH°_{ads} kJ mol ⁻¹	ΔS°_{ads} J mol ⁻¹ K ⁻¹
20	5.68	-37.35		126.74
40	5.78	-39.92	0.68	126.73
60	5.87	-42.50		126.73
80	5.96	-45.07		126.74

3.4. Potentiodynamic polarization curves

Fig. 11 shows the potentiodynamic polarization curves for C-steel in 1.0 M HCl in the devoid of and containing of different concentrations of synthesized cationic surfactant. Both the anodic and cathodic reactions of C-steel with acid can be seen inhibited in the presence of the cationic surfactant molecule.

Thus, the presence of cationic surfactant molecule diminishes the dissolution of C-steel as well as minimize the hydrogen evolution reaction. Table 5 displays the obtained corrosion parameters, E_{corr} , anodic Tafel slopes (β_a), cathodic Tafel slopes (β_c) and corrosion current density (i_{corr}) are recorded in Table 1. In this case, the inhibition efficiency η_p was evaluated from the equation (13) [50]:

$$\eta_p = \frac{i_{corr.} - i_{corr.(inh)}}{i_{corr.}} \times 100 \tag{13}$$

where $i_{corr.}$ and $i_{corr.(inh)}$ are the corrosion current densities for C-steel electrode without and with the presence of cationic surfactant.

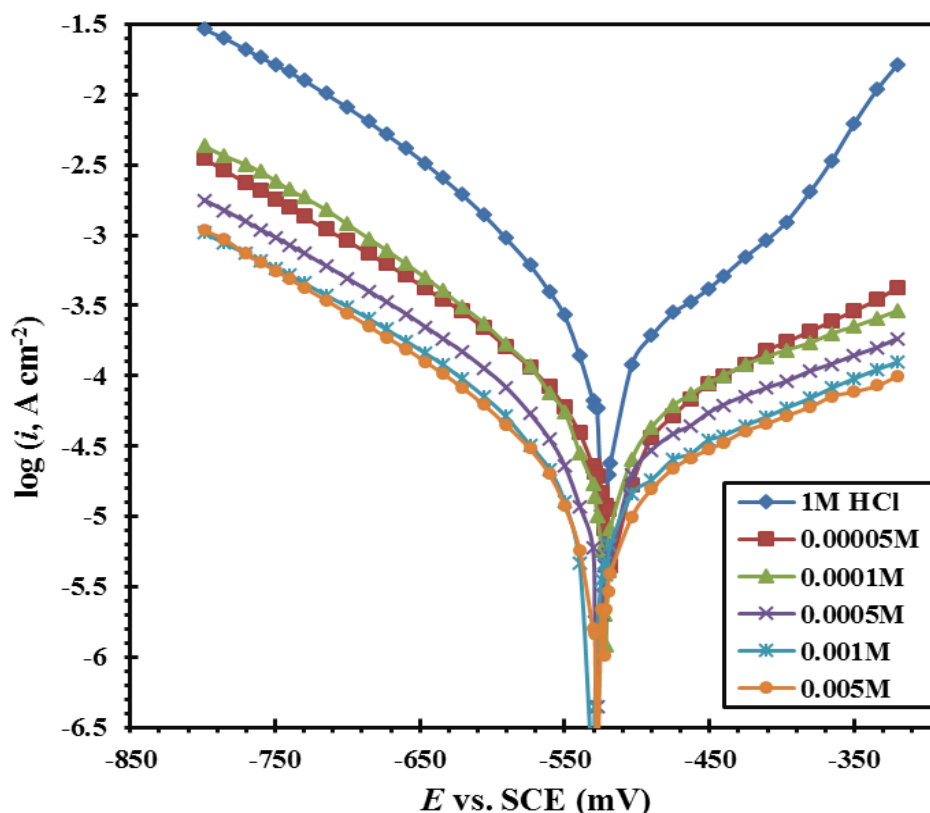


Figure 11. Potentiodynamic polarization curves for the C-steel in 1M HCl in the absence and presence of different concentrations of cationic surfactant at scanning rate 2mV s^{-1} .

Table 5 shows that the values of β_c and β_a have changed slightly; indicating that the mechanism of C-steel corrosion does not alter. By increasing the concentration of the cationic surfactant, the values of i_{corr} are lowered due to the adsorption of it on the C-steel surface. The values

of inhibition efficiency increase with the inhibitor concentration. The value of E_{corr} is nearly constant. The shift in $E_{\text{corr}} \leq 7$ by comparing the values of E_{corr} of the inhibited sample with the E_{corr} of the uninhibited sample suggested that the cationic surfactant molecule is a mixed type of inhibitor[51,52].

It is clear that there is a good correlation between the values of η_w and η_p obtained from weight loss and potentiodynamic polarization measurements.

Table 5. Potentiodynamic polarization parameters for C-steel corrosion in 1.0 M HCl in the absence and presence of different concentrations of the synthesized cationic surfactant at 20 °C

Conc. of inhibitor M	E_{corr} mV(SCE)	i_{corr} mA cm ⁻²	β_a mV dec ⁻¹	β_c mV dec ⁻¹	η_p %
0.00	-523.0	0.4241	186.2	-155.1	00
5x10 ⁻⁵	-518.5	0.0707	262.2	-166.2	83.33
1x10 ⁻⁴	-521.5	0.0588	296.4	-133.9	86.14
5x10 ⁻⁴	-527.5	0.0399	329.6	-159.3	90.58
1x10 ⁻³	-530.5	0.0343	398.5	-177.2	91.92
5x10 ⁻³	-527.5	0.0229	334	-159.0	94.60

3.5. Electrochemical impedance spectroscopy measurements

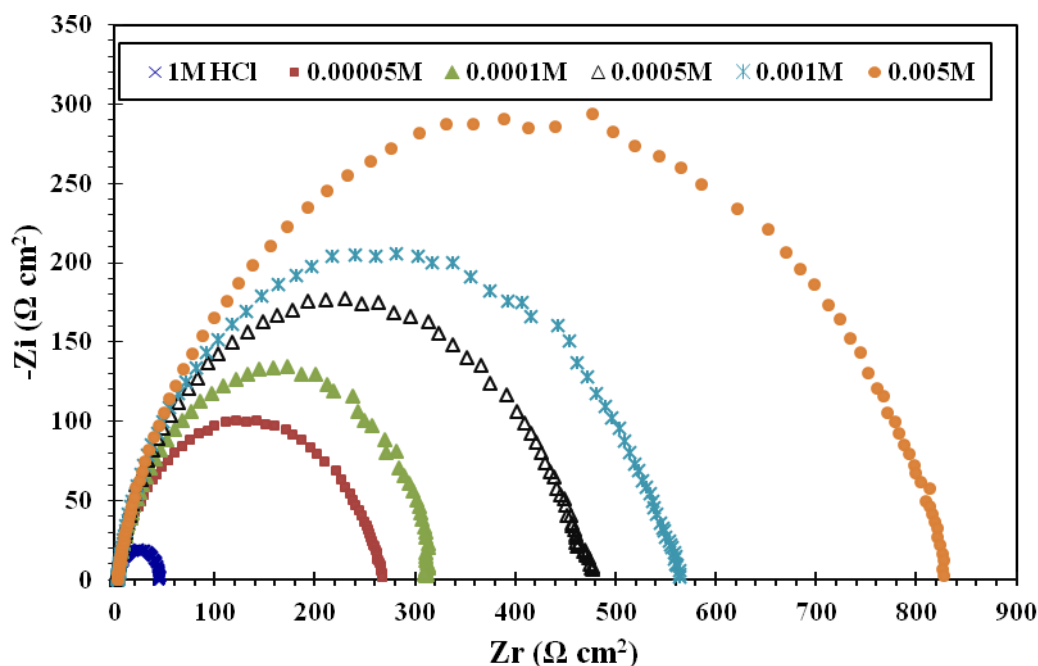


Figure 12. Nyquist plots for the C-steel in 1M HCl in the absence and presence of different concentrations of cationic surfactant.

The Nyquist diagram obtained using 1M HCl showed only one capacitive loop and increased semicircle diameter with increased cationic surfactant concentration indicating that the inhibitory film formed was enhanced by the addition of inhibitors as shown in Figure 12.

All the plots obtained showed only one semicircle and they were fitted using a fixed constant model once (Model Randall Fig.13). Bode plots (Fig. 14) showed that the addition of an inhibitor causes an increase in the interfacial impedance, which further increases upon increasing concentration of the inhibitor. At intermediate frequency, one peak only appeared in the phase-angle plots indicates a single time constant for the corrosion process at the metal–solution interface. All the major parameters derived from the impedance technique using the equivalent circuit are given in Table 6.

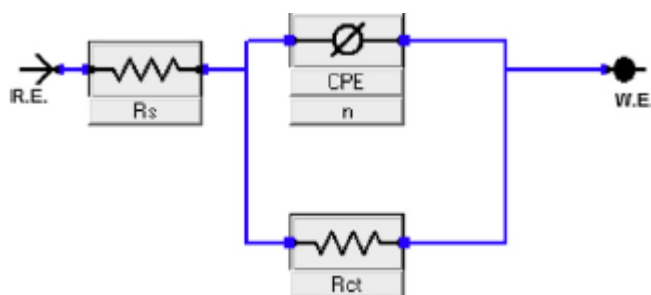


Figure 13. Electrical equivalent circuit used for modeling the interface C-steel /1 M HCl solution without and with the cationic surfactant.

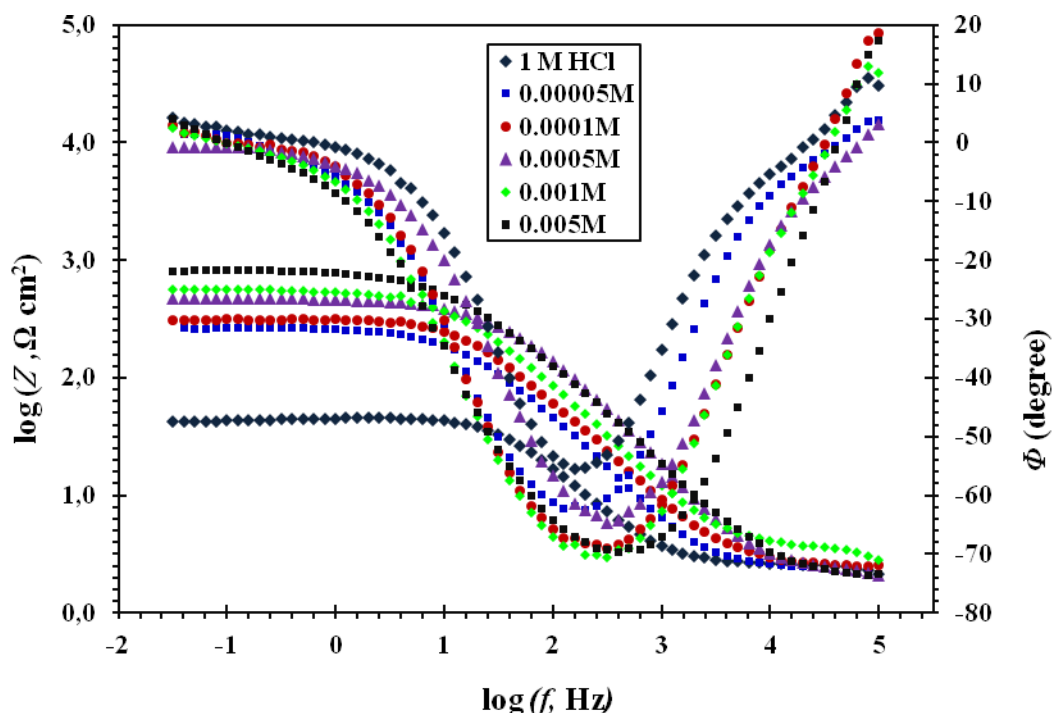


Figure 14. Bode plots of C-steel in 1M HCl in presence of different concentrations of cationic surfactant.

Table 6. Electrochemical impedance spectroscopy parameters for corrosion of C-steel in 1.0 M HCl in the absence and presence of different concentrations of the synthesized cationic surfactant at 20 °C

Conc. of inhibitor M	R_s $\Omega \text{ cm}^2$	Q_{dl} ($\Omega^{-1} \text{ s}^n \text{ cm}^{-2}$)	n	Error of n	R_{ct} $\Omega \text{ cm}^2$	C_{dl} $\mu\text{F cm}^{-2}$	η_I %
0.00	2.55	0.0001606	0.91	0.79	42.48	102.2	--
5×10^{-5}	2.32	0.0000843	0.87	0.47	259.6	48.06	83.64
1×10^{-4}	2.67	0.0000521	0.89	2.76	313.3	32.23	86.44
5×10^{-4}	2.29	0.0000407	0.88	0.51	454.4	24.31	90.65
1×10^{-3}	3.50	0.0000359	0.88	0.60	541.2	25.61	92.15
5×10^{-3}	3.24	0.0000319	0.85	0.72	796.7	19.20	94.67

The values of capacitance of double layer (C_{dl}) derived from fixed phase element (CPE) parameters using the following equation [30]:

$$C_{dl} = Q(\omega_{max})^{1-n} \quad (14)$$

where Q is the CPE constant, ω_{max} is the angular frequency in rad. S^{-1} , $\omega = 2\pi f_{max}$, (where f is the frequency at which the imaginary component of the impedance is maximum), i is the imaginary number and n is a CPE exponent which can be used as a gauge of the heterogeneity or roughness of the surface [52]. The value of n has the range of $0 \leq n \leq 1$. If the electrode surface is homogeneous and plane, the value of n equals to 1 and the metal-solution interface acts as a capacitor with regular surface [53].

The values of n were in the range from 0.85 to 0.91, indicating non-ideal capacitive behavior.

The inhibition efficiency (η_z) was calculated from the following equation:

$$\eta_z = \frac{R_{ct} - R_{ct}^0}{R_{ct}} \times 100 \quad (15)$$

where R_{ct}^0 and R_{ct} are the charge-transfer resistance values without and with inhibitor, respectively.

For a deviation from an ideal circular shape, it is often known as frequency dispersion, due to the surface roughness and the heterogeneity of the solid surface [54] The change of R_{ct} values according to the gradual replacement of the water molecules by the cationic surfactant molecules on the surface of the C-steel and thus to the reduced the number of active sites required for the corrosion reaction. Furthermore, the values of C_{dl} were decreased with increased cationic surfactant concentrations. The decrease in C_{dl} may be due to the low local dielectric constant and/ or the increase in the thickness of the protective layer on the surface of the electrode, thus enhancing the corrosion resistance of the studied C-steel

4. CONCLUSIONS

1. The synthesized novel cationic surfactant is effective inhibitor for corrosion of C-steel in 1 M HCl solution.
2. Novel cationic surfactant works as a mixed-type inhibitor.

3-The good inhibition efficiency of the novel cationic surfactant was interpreted by its adsorption on the C-steel surface and formation of a protective film.

4. The adsorption of novel cationic surfactant on C-steel surface obeys Langmuir isotherm.

5-Thermodynamic parameters indicate that the cationic surfactant is strongly adsorbed on C-steel surface.

References

1. C. M. Anbarasi and S. Rajendran, *Int. J. Curr. Eng. Tech.*, 3 (2013) 2088.
2. P. Rajeev, A.O. Surendranathan, Ch. S. N. Murthy, *J. Mater. Environ. Sci.*, 3 (2012) 856.
3. N.O. Eddy, F. Awe, E.E. Ebenso, *Int. J. Electrochem. Sci.*, 5 (2010) 1996.
4. M. Abdallah, H.M. Altass, B.A. AL Jahdaly, A.S. Fouda, *J Mol. Liq.*, 216 (2016) 590.
5. B.A. AL Jadedly, I.I. Althagafi, M. Abdallah, K.S. Khairou, S.A. Ahmed, *J. Mater. Environ. Sci.*, 7 (2016) 1798.
6. A. Zarrouk, B. Hammouti, T. Lakhliifi, M. Traisnel. H. Vezin, F. Bentiss, *Corros. Sci.*, 90 (2015) 572.
7. M. Abdallah, Sh.T. Atwa, N.M. Abdallah, I.M. El-Naggar, A.S. Fouda, *Anti Corros Meth. Mater.*, (2011) 31.
8. R.S. Abdel Hameed, M. Abdallah, *Prot. Met. Phys. Chem. Surf.*, 54 (2018) 113.
9. M. Abdallah, A.Y. El-Etre, M.G. Soliman, *Anti Corros Meth. Mater.*, 53 (2006) 118.
10. M.H.O. Ahmed, A.A. Al-Amiery, Y.K. Al-Majedy, A.H. Kadhum, A. Mohamad, T.S. Gaaz, *Res. in Phys.*, 8(2018) 728.
11. M. Abdallah, M.M. Salem, B.A. AL Jahdaly, M.I. Awad, E. Helal, A.S. Fouda, *Int. J. Electrochem. Sci.*, 12 (2017) 4543.
12. M. Abdallah, A.M. El-Dafrawy, M. Sobhi, A.H.M. Elwahy, M.R. Shaaban, *Int. J. Electrochem Sci.* 9 (2014) 2186.
13. H.J. Habeeb, H.M. Luaibi, R.M. Dakhil, A.H. Kadhum, T.S. Gaaz, *Res. Phys.*, 8 (2018) 1260.
14. A.S. Fouda, M. Abdallah, S.M. Al-Ashry, A.A. Abdel-Fattah, *Deasination*, 250 (2010) 538.
15. A.S. Fouda, M. Abdallah, A. Attia, *Chem. Eng. Comm.*, 197 (2010) 1091.
16. M. Abdallah, *Mater. Chem. Phys.*, 82 (2003) 786.
17. M.A. Deyab, *J. Mol. Liq.*, 255 (2018) 550.
18. Q. Zhang, Z. Gao, F. Xu, X. Zou, *Coll. Surf. A: Phys. Eng. Aspects*, 380 (2011) 191.
19. M. Sobhi, R. El-Sayed, M. Abdallah, *J. Surf. Deter.*, 16 (2013) 937.
20. O.A. Hazzazi, M. Abdallah, E.A.M. Gad, *Int. J. Electrochem. Sci.*, 9 (2014) 2237.
21. M. Abdallah, B.A.AL Jahdaly, M. Sobhi, A.I. Ali, *Int. J. Electrochem. Sci.*, 10 (2015) 4482.
22. M. Abdallah, B.A.AL Jahdaly, O.A. Al-Malyo, *Int. J. Electrochem. Sci.*, 10 (2015) 2740.
23. A. Fawzy, I.A. Zaaferany, H.M. Ali, M. Abdallah, *Int. J. Electrochem. Sci.*, 13 (2018) 4575.
24. M. Abdallah, *Annali Di Chimica*, 84 (1994) 529.
25. M. Sobhi, R. El-Sayed, M. Abdallah, *Chem. Eng. Comm.*, 203 (2016) 758.
26. M.A. Hegazy, M. Abdallah, H. Ahmed, *Corros. Sci.*, 52 (2010) 2897.
27. M. Abdallah, S.T. Atwa, M.M. Salem, A.S. Fouda, *Int. J. Electrochem. Sci.*, 8 (2013) 10001.
28. R.J. Meakins, *J. Appl. Chem.*, 13 (2007) 339.
29. M.A. Hegazy, H.M. Ahmed, A.S. El-Tabei, *Corros. Sci.*, 53 (2011) 671.
30. M.A. Hegazy, M. Abdallah, M.K. Awad, M.T.S. Rezk, *Corros. Sci.*, 81 (2014) 54.
31. M.A. Deyab, *Corros. Sci.*, 80 (2014) 359.
32. X. Wang, Y. Wan, Y. Gu, Y. Ma, F. Shi, M. Niu, Q. Wang, *Int. J. Electrochem. Sci.*, 9 (2014) 1840.
33. N.A. Negm, Y.M. Elkholy, M.K. Zahran, S.M. Tawfik, *Corros. Sci.*, 52 (2010) 3523.
34. S.K. Shukla, A.K. Singh, M.A. Quraishi, *Int. J. Electrochem. Sci.*, 6 (2011) 5779.

35. J. Zhang, W.W. Song, D.L.L. Shi, W. Niu, C.J. Li, M. Du, *Proc. Org. Coat.*, 75 (2012) 284.
36. J. Al-Fahemia, M. Abdallah, E.A.M. Gad, B.A. AL Jahdaly, *J Mol. Liq.*, 222 (2016) 1157.
37. A. Popova, E. Sokolova, S. Raicheva, M. Christov, *Corros. Sci.*, 45 (2003) 33
38. O.A. Hazazi, M. Abdallah, *Int. J. Electrochem. Sci.*, 8 (2013) 8138.
39. D.B. Hmamou, A. Zarrouk, R. Salghi, H. Zarrok, E.E. Ebenso, B. Hammouti, M.M. Kabanda, N. Bencha, O. Benali, *Int. J. Electrochem. Sci.*, 9 (2014) 120.
40. H.M. Bhajiwala, R.T. Vashi, *Bull. Electrochem.*, 17 (2001) 441.
41. D. Schweinsberg, G. George, A. Nanayakkara, D. Steinert, *Corros. Sci.*, 28 (1988) 33.
42. M. Sobhi, M. Abdallah, K.S. Khairou, *Monatsh fur Chemie*, 143 (2012) 1379.
43. D.B. Hmamou, R. Salghi, A. Zarrouk, H. Zarrok, B. Hammouti, S.S. Al-Deyab, M. Bouachrine, A. Chakir, M. Zougagh, *Int. J. Electrochem. Sci.*, 7 (2012) 5716.
44. K. Boumhara, F. Bentiss, M. Tabyaoui, J. Costa, J.M. Desjobert, A. Bellaouchou, A. Guenbour, B. Hammouti, S.S. Al-Deyab, *Int. J. Electrochem. Sci.*, 9 (2014) 1187.
45. M.A. Hegazy, *Corros. Sci.*, 51 (2009) 2610.
46. A.M. Badiea, K.N. Mohana, *Corros. Sci.*, 51 (2009) 2231.
47. M.P. Desimone, G. Gordillo, S.N. Simison, *Corros. Sci.*, 53 (2011) 4033.
48. M. Scendo, J. Trela, *Int. J. Electrochem. Sci.*, 8 (2013) 11951.
49. M. Şahin, S. Bilgiç, H. Yılmaz, *Appl. Surf. Sci.*, 195 (2002) 1.
50. A. Zarrouk, H. Zarrok, R. Salghi, N. Bouroumane, B. Hammouti, S.S. Al-Deyab, R. Touzani, *Int. J. Electrochem. Sci.*, 7 (2012) 10215.
51. E.S. Ferreira, C. Giancomelli, F.C. Giacomelli, A. Spinelli, *Mater. Chem. Phys.*, 83 (2004) 129.
52. W.H. Li, Q. He, C.L. Pei, B.R. Hou, *J. Appl. Electrochem.*, 38 (2008) 289.
53. W.E. Amira, A.A. Rahim, H. Osman, K. Awang, P.B. Raja, *Int. J. Electrochem. Sci.*, 6 (2011) 2998.
54. J.W. Lenderink, M. Linden, J.H. Wit, *Electrochim. Acta*, 38 (1993) 1989.

© 2018 The Authors. Published by ESG (www.electrochemsci.org). This article is an open access article distributed under the terms and conditions of the Creative Commons Attribution license (<http://creativecommons.org/licenses/by/4.0/>).